3-2006

Kinetic and Spectroscopic Characterization of the E134A- and E134D-altered *dapE*-encoded *N*-succinyl-l,l-diaminopimelic acid desuccinylase from *Haemophilus influenzae*

Ryan S. Davis
Utah State University

David L. Bienvenue
Utah State University

Sabina I. Swierczek
Utah State University

Danuta M. Gilner
Utah State University

Lakshman Rajagopal
Utah State University

See next page for additional authors

JBIC Journal of Biological Inorganic Chemistry, Vol. 11 (March 2006): 206–216. DOI.

Kinetic And Spectroscopic Characterization Of The E134A- And E134D-Altered *DapE*-Encoded *N*-Succinyl-L,L-Diaminopimelic Acid Desuccinylase From *Haemophilus Influenzae*

Ryan Davis
Department of Chemistry and Biochemistry, Utah State University, Logan, UT
David Bienvenue
Department of Chemistry and Biochemistry, Utah State University, Logan, UT
Sabina I. Swierczek
Department of Chemistry and Biochemistry, Utah State University, Logan, UT
Danuta M. Gilner
Department of Chemistry and Biochemistry, Utah State University, Logan, UT
Lakshman Rajagopal
Department of Chemistry and Biochemistry, Utah State University, Logan, UT

Brian Bennett
National Biomedical EPR Center, Department of Biophysics, Medical College of Wisconsin, Milwaukee, WI
Richard C. Holz
Department of Chemistry and Biochemistry, Utah State University, Logan, UT

Abstract

Glutamate-134 (E134) is proposed to act as the general acid/base during the hydrolysis reaction catalyzed by the *dapE*-encoded *N*-succinyl-L,L-diaminopimelic acid desuccinylase (DapE) from *Haemophilus influenzae*. To date, no direct evidence has been reported for the role of E134 during catalytic turnover by DapE. In order to elucidate the catalytic role of E134, altered DapE enzymes were prepared in which E134 was substituted with an alanine and an aspartate residue. The Michaelis constant (K_m) does not change upon substitution with aspartate but the rate of the reaction changes drastically in the following order: glutamate (100% activity), aspartate (0.09%), and alanine (0%). Examination of the pH dependence of the kinetic constants k_{cat} and K_m for E134D-DapE revealed ionizations at pH 6.4, 7.4, and approximately 9.7. Isothermal titration calorimetry experiments revealed a significant weakening in metal K_d values of E134D-DapE. D134 and A134 perturb the second divalent metal binding site significantly more than the first, but both altered enzymes can still bind two divalent metal ions. Structural perturbations of the dinuclear active site of DapE were also examined for two E134-substituted forms, namely E134D-DapE and E134A-DapE, by UV–vis and electron paramagnetic resonance (EPR) spectroscopy. UV–vis spectroscopy of Co(II)-substituted E134D-DapE and E134A-DapE did not reveal any significant changes in the electronic absorption spectra, suggesting that both Co(II) ions in E134D-DapE and E134A-DapE reside in distorted trigonal bipyramidal coordination geometries. EPR spectra of [Co_(E134D-DapE)] and [Co_(E1341A-DapE] are similar to those observed for [CoCo(DapE)] and somewhat similar to the spectrum of $[Co(H_2O)_6]^{2+}$ which typically exhibit E/D values of approximately 0.1. Computer simulation returned an axial g-tensor with $g_{(x,y)}$=2.24 and E/D=0.07; g_z was only poorly determined, but was estimated as 2.5–2.6. Upon the addition of a second Co(II) ion to [Co_(E134D-DapE)] and [Co_(E134A-DapE)], a broad axial signal was observed; however, no signals were observed with $\boldsymbol{B}_0 || \boldsymbol{B}_1$ (“parallel mode”). On the basis of these data, E134 is intrinsically involved in the hydrolysis reaction catalyzed by DapE and likely plays the role of a general acid and base.

Introduction

According to recent estimates from the United States Centers for Disease Control and Prevention (the CDC), more than ten million people died worldwide from bacterial infections in 1995 [1]. Tuberculosis, for example, is the leading cause of death in adults by an infectious disease [2]. The importance of developing new drugs to fight infectious disease, such as tuberculosis, is underscored by the emergence of several pathogenic bacterial strains that are resistant to all currently available antibiotics [1, 3–5]. In order to overcome bacterial resistance to antibiotics, new enzyme targets must be located and small-molecule inhibitors developed. The *meso*-diaminopimelate (mDAP)/lysine biosynthetic pathway offers several potential antibacterial targets that have yet to be explored [6–8]. Since both products of this pathway, mDAP and lysine, are essential components of the peptidoglycan cell wall in Gram-negative and some Gram-positive bacteria, inhibitors of enzymes within this pathway may provide a new class of antibiotics [4]. The fact that there are no similar pathways in mammals suggests that inhibitors of enzymes in the mDAP/lysine pathway will provide selective toxicity against bacteria and potentially have little or no effect on humans.

One of the enzymes in this pathway [9], the *dapE*-encoded *N*-succinyl-L,L-diaminopimelic acid desuccinylase (DapE), catalyzes the hydrolysis of *N*-succinyl-L,L-diaminopimelate (L,L-SDAP) to L,L-diaminopimelate and succinate [10]. It has been shown that deletion of the gene encoding DapE is lethal to *Helicobacter pylori* and *Mycobacterium smegmatis* [11, 12]. Even in the presence of lysine-supplemented media, the DapE deletion cell line of *H. pylori* was unable to grow; therefore, DapEs are essential for cell growth and proliferation. DapEs have been purified from *Escherichia coli* and *Haemophilus influenzae*, while the genes that encode for DapEs have been sequenced from several bacterial sources such as *Corynebacterium glutamicum*, *H. pylori*, and *M. tuberculosis*. The DapEs from *E. coli* and *H. influenzae* have been overexpressed in *E. coli* and purified to homogeneity [10, 13]. Both of these DapEs are small, dimeric enzymes (41.6 kDa per subunit) that require 2 g atom of zinc per mole of polypeptide for full enzymatic activity [7, 10]. Sequence alignment of the DapE from *H. influenzae* with the aminopeptidase from *Aeromonas proteolytica* (AAP) and the structurally related carboxypeptidase G_2 from *Pseudomonas* sp. strain RS-16 (CPG_2) indicated that all of the amino acids that function as metal ligands in AAP and CPG_2 are strictly conserved in DapE [10]. However, it should be noted that no catalytically important amino acid residues have been identified for DapE to date.

Comparison of all known crystallographically characterized metallohydrolases, including AAP and CPG_2, reveals some common features for both mononuclear and dinuclear hydrolases [14–17]. All have at least one bound water molecule and many contain an active-site carboxylate residue that does not function as a metal ligand. This carboxylate residue, usually a glutamate, often forms a hydrogen bond to a water molecule that is also bound to an active-site metal ion. The X-ray crystal structure of AAP reveals that an oxygen atom of glutamate-151 (E151) forms a hydrogen bond with a water molecule that bridges between the two Zn(II) ions [18]. E151 was recently shown to act as the proton shuttle during catalytic turnover [19]. On the basis of sequence alignment between DapE and AAP, glutamate-134 (E134) was proposed to function in an identical manner in DapE enzymes as E151 in AAP [10]. In order to gain an understanding of the catalytic role of E134 in the hydrolysis of *N*-succinyl-L,L-diaminopimelic acid, we prepared the E134A- and E134D-altered DapE enzymes and characterized each by kinetic and spectroscopic methods. These data indicate that E134 is intimately involved in catalysis and likely functions as the general acid/base.

Materials and methods

Reagents

D,L-*α*,*ε*-DAP (98% pure), succinic anhydride, and ion-exchange resin (Dowex 50WX8–200, H^+ form) were purchased from Sigma. Technically pure 2-naphthalenesulfonic acid (70%) was purchased from Aldrich, crystallized from a 5% aqueous solution of HCl, and dried in a vacuum desiccator over $CaCl_2$ to give a white solid of 2-naphthalenesulfonic acid 1-hydrate, melting point 397–398 K (confirmed by NMR). Microcrystalline cellulose was purchased from EM Science. All solvents and additional chemicals were purchased from either Sigma or Fisher Scientific.

Protein expression and purification

The recombinant DapE from *H. influenzae* was expressed and purified, as previously described with minor modifications, from a stock culture kindly provided by John Blanchard [10]. Briefly, approximately 12 g of cell paste was suspended in 50 mL of 10 mM *N*-tris(hydroxymethyl)methylglycine (Tricine) buffer, pH 7.8, containing four protease inhibitor tablets (complete protease inhibitor tables, Boehringer Mannheim). Lysozyme (10 mg) was added to the mixture and stirred for 30 min at 277 K. Cells were lysed by sonication (Heat Systems-Ultrasonics) at 1-min intervals, four repetitions, and the cell debris was removed by centrifugation for 40 min at 12,000*g*. DNase (2 mg) was added and after approximately 20 min of incubation, the solution was loaded onto a fast-flow Q-sepharose anion-exchange column that had been pre-equilibrated with 10 mM Tricine buffer, pH 7.8. A flow rate of 3 mL min^{-1} was used and a 600-min linear gradient of NaCl (0.2–0.5 M) was used to elute

DapE. DapE activity was detected between 0.25 and 0.3 M NaCl. The active fractions were concentrated using an Amicon YM-10 membrane. Purified DapE from *H. influenzae* exhibited a single band on sodium dodecyl sulfate–polyacrylamide gel electrophoresis, indicating M_r=41,500. Protein concentrations were determined from the absorbance at 280 nm using a molar absorptivity calculated using the method developed by Gill and Hippel [20] (ε_{280}=36,040 M^{-1} cm^{-1}). The protein concentration determined using this molar absorptivity was in close agreement to that obtained using a Bradford assay. Individual aliquots of purified DapE were stored in liquid nitrogen until needed.

Site-directed mutagenesis

Site-directed mutants were obtained using the Quick Change Site-Directed Mutagenesis Kit (Stratagene, La Jolla, CA, USA) following the procedure outlined by Stratagene. The following primers were used: 5′-GCA TTA TTG ATT ACC TCT GAT XXX GAG GCT ACC GC-3′ and 5′-GC GGT AGC CTC YYY ATC AGA GGT AAT CAA TAA TGC-3′ with GCT and GAC for XXX and AGC and GTC for YYY to prepare E134A- and E134D-altered DapE enzymes, respectively. Reaction products were transformed into *E. coli* XL1-Blue competent cells, grown on Luria–Bertani agarose plates containing ampicillin (100 μg mL^{-1}). A single colony of each mutant was grown in 100 mL Luria–Bertani medium containing 100 μg mL^{-1} ampicillin. Plasmids were isolated using the QIAprep-Spin Miniprep Kit (QIAGEN, Valencia, CA, USA). Each mutation was confirmed by DNA sequencing (USU Center for Integrated BioSystems). Plasmids containing the altered DapE genes were transformed into *E. coli* BL21 Star (DE3) cells (Invitrogen, Carlsbad, CA, USA).

Metal content measurements

Apo-DapE was prepared by extensive dialysis for 3–4 days against 10 mM EDTA in 50 mM 4-(2-hydroxyethyl)-1-piperazineethanesulfonic acid (HEPES) buffer, pH 7.5. DapE was then exhaustively dialyzed against metal-free (chelexed) 50 mM HEPES buffer, pH 7.5. Any remaining metal ions were estimated by comparing the activity of the apo-enzyme with a sample that had been reconstituted with Zn(II). DapE incubated with EDTA typically had less than 5% residual activity after dialysis. Apo-DapE samples were incubated with $ZnCl_2$ (99.999%; Strem Chemicals, Newburyport, MA, USA) for 30 min prior to exhaustive dialysis into Chelex-treated buffer as previously reported [21].

Synthesis of *N*-succinyl-diaminopimelic acid

The D,D and L,L isoforms of DAP were separated from the D,L isoform using the method described by Bergmann and Stein [22]. *N*-succinyl-diaminopimelic acid (SDAP) was synthesized using the procedure described by Lin et al. [23], providing an overall yield of 41% (1.84 g; 5.7 mmol) [24]. NMR (270 MHz, D_2O, δ, ppm): 1.25–1.45 (m, 2H), 1.55–1.90 (m, 4H), 2.29–2.52 (m, 4H), 3.64 (dd, 1H), 4.05 (dd, 1H), 4.76 (bs, H_2O + ammonium ion). The L,L-SDAP and *N*-succinyl-D,D-diaminopimelate (D,D-SDAP) isoforms were separated using an high-performance liquid chromatograph (Shimadzu SCL-10A VP) with a Chirobiotic T column (250 mm × 10 mm; Alltec). The isocratic mixture of 20% methanol in water (adjusted to pH 4) was used as the eluting solvent. The two isoforms were present in an approximate 1:1 ratio.

Enzymatic assay of DapE

The specific activity of E134A-DapE and E134D-DapE was determined by monitoring amide bond cleavage of L,L-SDAP at 215 nm in 50 mM HEPES buffer, pH 7.5, in the presence of 3 equiv Zn(II). The kinetic parameters V_{max} (velocity) and K_m (Michaelis constant) were determined at pH 7.5 by quantifying the amide bond cleavage (decrease in absorbance) of L,L-SDAP at 225 nm (ε=698 M^{-1} cm^{-1}) in triplicate. Enzyme activities are expressed as units per milligram, where one unit is defined as the amount of enzyme that releases 1 μmol of L,L-SDAP at 303 K in 1 min. Catalytic activities were determined with an error of ±10%. Initial rates were fit directly to the Michaelis–Menten equation to obtain the catalytic constants K_m and k_{cat}.

Kinetic characterization of DapE with various divalent transition metal ions [Mn(II), Mg(II), Co(II), Ni(II), Cu(II), Zn(II), Cd(II)] in the active site was performed by placing apo-DapE in the presence of 100 μM ultrapure metal (99.999%; Strem Chemicals). After 1-h incubation period, the activity of metal-substituted DapE was determined by monitoring the hydrolysis of the substrate mixture D,D-, L,L-SDAP.

Isothermal titration calorimetry

Isothermal titration calorimetry measurements were carried out using a MicroCal OMEGA ultrasensitive titration calorimeter at 298±0.2 K. Association constants (K_b) were obtained by fitting these data, after subtraction of the background heat of dilution, via an interactive process using the Origin software package. This software package uses a nonlinear least-squares algorithm which allows the concentrations of the titrant and the sample to be fit to the heat flow per injection by an equilibrium binding equation for two noninteracting sites. The K_b value, enzyme–metal stoichiometry (n), and the change in enthalpy (ΔH^0) were allowed to vary during the fitting process. The divalent metal ion titrants and apo-enzyme solutions were prepared in chelexed HEPES buffer at pH 7.5. Stock buffer solutions were thoroughly degassed before each titration. The enzyme solution (60–90 μM) was placed in the calorimeter cell and stirred at 200 rpm to ensure rapid mixing. Typically, 4–6 μL of titrant was delivered over 7.6 s with a 6-min interval between injections to allow for complete equilibration. Each titration was continued until 4.5–6 equiv M(II) had been added to ensure that no additional complexes were formed in excess titrant. A background titration, consisting of the identical titrant solution but only the buffer solution in the sample cell, was subtracted from each experimental titration to account for heat of dilution. The heat of reaction measured during the experiment was converted into association constants (K_a) using the Gibbs free-energy relationship:

$$\Delta G^0 = -RT\ln\left(K_a\right) = \Delta H^0 - T\Delta S^0,$$

(1)

where R=1.9872 cal mol^{-1} K^{-1}. The relationship between K_a and K_d is defined as

$$K_d = 1/K_a.$$

(2)

pH profiles

The enzymatic activities of DapE and the E134D form of DapE at pH values between 6.0 and 9.0 were measured using L,L-SDAP as the substrate. The conditions and methods used were identical to those described by Javid-Majd and Blanchard [25]. Briefly, the concentration of each buffer used was 50 mM and the following buffers were used: phosphate (pH 6.0–8.0) and tris(hydroxymethyl)aminomethane (Tris) (pH 8.0–9.0). No additional Zn(II) was included in any of the buffers listed above pH 8.0; however, between pH 6.0 and 8.0, 0.1 mM Zn(II) was included in all the buffers. The kinetic parameters k_{cat}, K_m, and k_{cat}/K_m were determined using five to seven different substrate concentrations ranging from 0.67 to 3.0 times the observed K_m value at each pH studied. Overlapping points for each buffer used were collected and the resulting data matched within ±5%. Kinetic parameters and fits to the kinetic curves were obtained using Igor Pro (Wavemetrix, Lake Oswego, OR, USA) by fitting the experimental data to the appropriate equations.

Spectroscopic measurements

Electronic absorption spectra were recorded with a Shimadzu UV-3101PC spectrophotometer with protein concentrations of approximately 1 mM. All apo-DapE variant samples used in the spectroscopic measurements were made rigorously anaerobic prior to a 30-min incubation period with Co(II) ($CoCl_2$ purity 99.999% or greater; Strem Chemicals) at 273–298 K. All Co(II)-containing samples were handled throughout in an anaerobic glove

box (Ar/5% H_2, 1 ppm or less O_2; Coy Laboratories). Electronic absorption spectra were normalized for the protein concentration and the absorption due to uncomplexed Co(II) ($\varepsilon_{512\,nm}$=6.0 M^{-1} cm^{-1}). Low-temperature electron paramagnetic resonance (EPR) spectroscopy was performed using a Bruker ESP-300E spectrometer equipped with an ER 4116 DM dual mode X-band cavity and an Oxford Instruments ESR-900 helium-flow cryostat. Enzyme concentrations for EPR were approximately 1 mM. Background spectra recorded with a buffer sample were aligned with and subtracted from experimental spectra as in earlier work [26]. EPR spectra were recorded at microwave frequencies of approximately 9.65 GHz: precise microwave frequencies were recorded for individual spectra to ensure precise *g*-alignment. All spectra were recorded at 100-kHz modulation frequency. Other EPR running parameters are specified in the figure legends for individual samples. Each variant was incubated with the appropriate amount of Co(II) for 30 min at 298 K and then frozen in an EPR tube for analysis.

Results

Kinetic studies on altered DapE enzymes

The K_m and k_{cat} values for E134D-DapE were obtained by fitting the observed data to the Michaelis–Menten equation (Table 1). The k_{cat} value obtained for E134D-DapE was approximately 1,000 times lower than that for wild-type (WT) DapE (50 mM phosphate buffer, pH 7.6); however, the observed K_m value for E134D-DapE did not change significantly upon the substitution of the glutamate with aspartate. When E134 is replaced with a residue that cannot transfer a proton (E134A), no activity is observed.

Table 1 Kinetic data for wild-type (*WT*) *dapE*-encoded *N*-succinyl-L,L-diaminopimelic acid desuccinylase (*DapE*) and the glutamate-134 (*E134*) altered enzymes recorded at pH 7.5

	k_{cat} (s^{-1})	K_m (mM)	Specific activity (U mg^{-1})
WT DapE	140±10	0.73±0.05	180
E134D-DapE	0.13±0.01	0.65±0.05	0.17
E134A-DapE	ND	–	–

Activation of E134D-DapE by first-row transition metals

Activation of apo-E134D-DapE by several first-row divalent transition metals was examined [24]. Substrate hydrolysis (k_{cat}) of a 1.5 mM D,D-, L,L-SDAP buffered solution was monitored as a function of divalent metal ion concentration under anaerobic conditions (Fig. 1). Co(II) provides the most active E134D-DapE enzyme and is approximately 2 times more active than the Zn(II)-loaded form of DapE [10]. Interestingly, Mn(II) ions activate DapE but only approximately 20% of the Zn(II)-loaded DapE activity is observed. The relative ordering of the observed k_{cat} values for D,D-, L,L-SDAP hydrolysis is Co(II)>Zn(II)>Cd(II)>Mn(II). The activity of E134D-DapE was also tested with Ni(II), Cu(II), and Mg(II) ions present but no substrate hydrolysis was observed under the experimental conditions used.

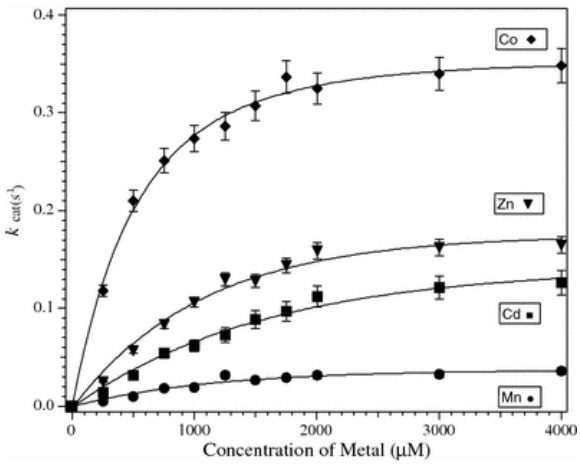

Fig. 1 Activity of a 6 μM sample of E134D–*dapE*-encoded *N*-succinyl-L,L-diaminopimelic acid desuccinylase (DAPE) in the presence of various divalent transition metal ions determined in 50 mM 4-(2-hydroxyethyl)-1-piperazineethanesulfonic acid (*HEPES*) buffer at pH 7.5. See "Site-directed mutagenesis" for an explanation of E134D

Isothermal titration calorimetry

The best fits obtained for the E134D-DapE and E134A-DapE altered enzymes provided *n* values of two for two noninteracting sites (Table 2). For WT DapE, Zn(II) and Co(II) bind tightly to the first metal binding site with dissociation constants (K_d) of 0.44±0.05 and 0.14±0.05 μM, respectively (S.I. Swierczek, S. Mitra, K. Baron, and R.C. Holz, unpublished results). On the other hand, the observed K_d values for Zn(II) binding to the first metal binding site of E134A-DapE and E134D-DapE are 0.62±0.05 and 1.3±0.5 μM, respectively (Fig. 2). For Co(II) binding to the first divalent metal binding sites of E134D-DapE and E134A-DapE, the observed K_d values are 0.028±0.005 and 0.094±0.005 μM, respectively (Fig. 3). On the other hand, the second metal binding site for WT DapE is significantly weaker for both Zn(II) (K_d=1.4±0.5 μM) and Co(II) (K_d=2.5±0.5 μM). For E134A-DapE and E134D-DapE, Zn(II) binding to the second metal binding sites exhibits K_d values of 65.4 and 9.1 μM, respectively. Similarly, for Co(II) binding to the second metal binding sites of E134A-DapE and E134D-DapE, the observed K_d values are 60.2±0.5 and 1.2±0.5 μM, respectively.

Table 2 Isothermal titration calorimetry data for the Zn(II)-loaded and Co(II)-loaded WT, E134A-DapE and E134D-DapE altered enzymes

	n	K_{a1}, K_{a2} (M^{-1})	K_{a1}, K_{a2} (μM)	ΔH^{0}_{1}, ΔH^{0}_{2} (kcal mol^{-1})	$T\Delta S^{0}_{1}$, $T\Delta S^{0}_{2}$ (kcal mol^{-1})	ΔG^{0}_{1}, ΔG^{0}_{2} (kcal mol^{-1})
[ZnZn(DapE)]	1.0	2.27×10^{5}	0.44	6.5	46	−7.3
	1.0	7.35×10^{4}	1.4	−3.4	10	−6.6
[CoCo(DapE)]	1.0	7.14×10^{5}	0.14	−3.4	18	−9.0
	1.0	4.00×10^{4}	2.5	6.5	48	−8.0
[ZnZn(E134D)]	1.0	7.88×10^{4}	1.3	0.30	7.0	−6.7
	1.1	1.10×10^{4}	9.1	21	26	−5.5
[CoCo(E134D)]	0.9	3.52×10^{6}	0.028	5.3	14	−8.9
	1.0	8.08×10^{4}	1.24	7.3	14	−6.7
[ZnZn(E134A)]	1.1	1.61×10^{5}	0.62	−0.21	6.9	−7.1
	1.1	1.56×10^{3}	65.4	61	66	−4.4
[CoCo(E134A)]	0.8	1.06×10^{6}	0.094	9.0	17	−8.2
	1.0	1.61×10^{3}	60.2	3.2	7.6	−4.4

See “Site-directed mutagenesis” for an explanation of E134A and E134D

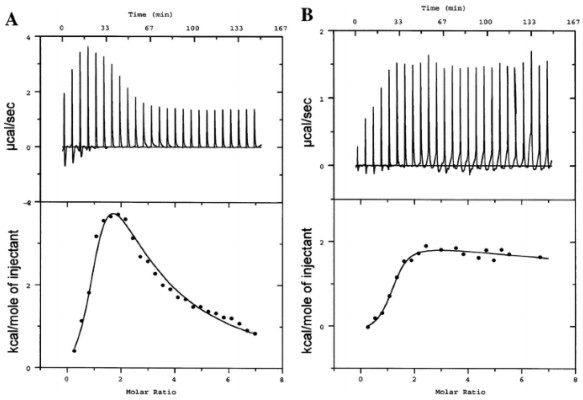

Fig. 2 Isothermal titration data for Zn(II) binding to the **a** E134D-DapE and **b** E134A-DapE enzymes in 50 mM HEPES buffer at pH 7.5. See “Site-directed mutagenesis” for an explanation of E134A

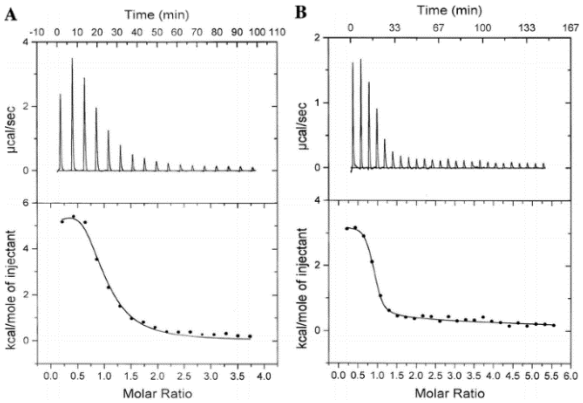

Fig. 3 Isothermal titration data for Co(II) binding to the **a** E134D-DapE and **b** E134A-DapE enzymes in 50 mM HEPES buffer at pH 7.5

pH dependence

The pH dependence of the kinetic parameters of E134D-DapE was investigated over the pH range 6.0–9.0. The E134D-DapE altered enzyme displayed optimum catalytic efficiency at pH values between 7.5 and 8.5 (Fig. 4). Activity below pH 6.0 was not observed and K_m values obtained above pH 9.0 were too large to measure with the current assay [10]. Phosphate (6.0–8.0) and Tris (8.5–9.0) buffers were used owing to their low absorbance at 215 nm. These kinetic data were plotted as log(parameter) versus pH and fit to Eq. 3:

$$\text{parameter} = c/(1 + [\text{H}^+]/K_1 + K_2/[\text{H}^+]), \quad (3)$$

where parameter is k_{cat} or k_{cat}/K_m and K_1 and K_2 are the respective ionization constants, while $[\text{H}^+]$ is the hydrogen ion concentration. The pH dependence of logK_m (Fig. 4, top curve) was obtained by subtracting plots of log(k_{cat}/K_m) from log(k_{cat}); thus, the inflection points reflect groups with ionizations at 6.4, 7.4, and approximately 9.7. The observed changes in k_{cat} are small over the pH range 7.0–9.0, but a sharp drop is observed below pH 7.0, with a single inflection at 6.4 (Fig. 4, middle curve). Plots of log(K_m) and log(k_{cat}/K_m) versus pH for E134D-DapE likely form bell-shaped curves but this assertion cannot be made conclusively owing to the lack of our ability to obtain data points above pH 9.0. Therefore, a plot of log(k_{cat}/K_m) versus pH reveals one inflection in the acidic range, at 7.3. An inflection in the basic range was estimated to be approximately 9.7 (Fig. 4, bottom curve).

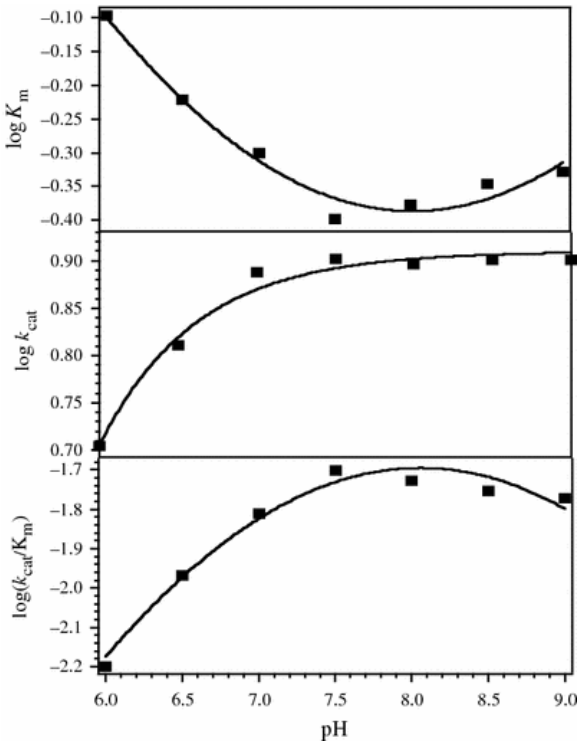

Fig. 4 pH dependence of the observed kinetic parameters for the hydrolysis of *N*-succinyl-L,L-diaminopimelate (*L , L -SDAP*)by Zn(II)-loaded E134D-DapE. *Top* pH dependence of K_m—obtained by subtraction of log(k_{cat}/K_m) from logk_{cat} (*solid line*); pK_{e1}=6.4, pK_{HS}=7.4, pK_{e2}=9.7. *Middle* pH dependence of logk_{cat}—fit to the experimental data using Eq. 3 (*solid line*); pK_{ES1}=6.4, pK_{ES2}=9.7. *Bottom* pH dependence of log(k_{cat}/K_m)—fit to the experimental data using Eq. 3 (*solid line*); pK_{HS}=7.4, pK_{e2}=9.7. Fits were obtained using Igor Pro (Wavemetrix). Error bars are smaller than the symbols used

Spectroscopic studies

Electronic absorption spectra of the E134A- and E134D-altered DapE enzymes were recorded in the presence of 1 and 2 equiv Co(II) ([Co_(E134A-DapE)], [CoCo(E134A-DapE)], [Co_(E134D-DapE)], and [CoCo(E134D-DapE)]). The addition of 1 equiv Co(II) to E134A-DapE provided a visible absorption spectrum with a maximum at 555 nm (ε_{555}=165 M^{-1} cm^{-1}) (Fig. 5). Addition of a second equivalent of Co(II) to E134A-DapE resulted in an increase in absorbance at 555 nm to 174 M^{-1} cm^{-1}, similar to the situation for WT DapE. Addition of 1 equiv Co(II) to E134D-DapE produced a visible absorption spectrum with a maximum at 556 nm (ε_{556}=187 M^{-1} cm^{-1}) (Fig. 5). Addition of a second equivalent of Co(II) to E134D-DapE increased the absorption intensity at 556 nm to 216 M^{-1} cm^{-1}.

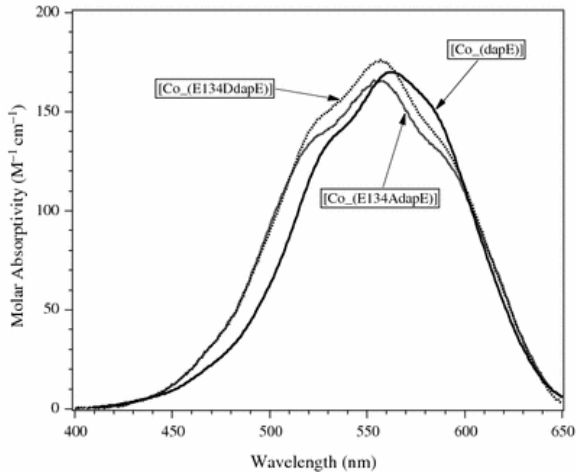

Fig. 5 Electronic absorption spectra of Co(II)-loaded E134A-DapE and E134D-DapE recorded after the addition of one equivalent of Co(II) in 50 mM HEPES buffer at pH 7.5

EPR spectra of [Co_(E134A-DapE)], [CoCo(E134A-DapE)], [Co_(E134D-DapE)], and [CoCo(E134D-DapE)] were recorded at several temperatures (3.5–70 K) and microwave powers (0.5–50 mW). EPR spectra of [Co_(E134D-DapE)], [Co_(DapE)], and [CoCo(DapE)] are presented in Fig. 6. Upon addition of 0.25–1.0 equiv Co(II) to apo-E134D-DapE or apo-E134A-DapE the spectra are similar to those observed for [CoCo(DapE)], AAP, the methionyl aminopeptidase from *E. coli* (*Ec*MetAP-I), and somewhat similar to $[Co(H_2O)_6]^{2+}$ which typically exhibit *E*/*D* values of approximately 0.1 [24, 26–28]. Computer simulation returned an axial *g*-tensor with $g_{(x,y)}$=2.24 and *E*/*D*=0.07; g_z was only poorly determined, but was estimated as 2.5–2.6. Upon the addition of a second Co(II) to [Co_(E134D-DapE)] and [Co_(E134A-DapE)], a broad axial signal was observed. Since the axial zero-field splitting is unknown and g_z is ill defined, calculation of the transition probability is not possible and thus accurate spin quantitation of the EPR-active Co(II) species is impossible. However, by direct comparison (peak height) with spectra from hexaaquo-Co(II), the spin concentrations of the spectra from [CoCo(E134A-DapE)] and [CoCo(E134D-DapE)] suggest approximately 2 mol of EPR-detectable Co(II) per mole of E134D-DapE and E134A-DapE. No signals were observed with $\boldsymbol{B}_0 || \boldsymbol{B}_1$ ("parallel mode").

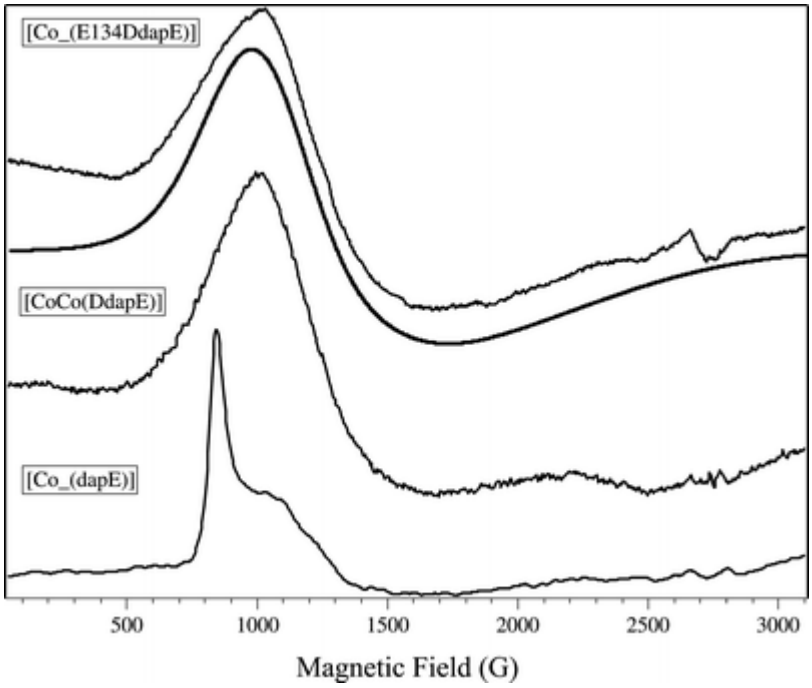

Fig. 6 Comparison of the electron paramagnetic resonance (*EPR*) spectra of Co(II)-loaded E134D-DapE recorded after the addition of 1 equiv Co(II) with [Co_(DapE)] and [CoCo(DapE)]. The *dashed line* indicates the simulation of the [Co_(E134D-DapE)] EPR spectrum with $g_{(x,y)}$=2.24 and *E*/*D*=0.07; g_z was only poorly determined, but was estimated as 2.5–2.6. All EPR spectra were recorded at 10 K using a microwave power of 0.2 mW in 50 mM HEPES buffer at pH 7.5

Discussion

Metalloproteases containing dinuclear active sites, such as DapE [29], are promising targets for drug discovery. DapE is a particularly attractive target for the development of a new class of antibiotics owing to its role in cell wall synthesis in bacteria; however, very little is known about how DapE catalyzes the hydrolysis of L,L-SDAP to L,L-diaminopimelate and succinate. Alignment of several gene sequences of DapE enzymes with CPG_2 and

AAP [10] indicated that all of the amino acids that function as metal ligands are strictly conserved, including a proposed nonligating amino acid E134. On the basis of these alignment data [10] and X-ray crystallographic data reported for AAP and CPG_2 [18, 30, 31], E134 corresponds to E151 in AAP. This amino acid residue was recently shown to function as both a general acid and a general base during catalysis [19]. E151 assists in deprotonating the metal-bound water molecule to a more nucleophilic hydroxo moiety, similar to that of glutamate-270 in carboxypeptidase A [32] and provides a proton to the newly formed N terminus of the outgoing peptide substrate. In order to determine the role of E134 in catalysis, we prepared the DapE-altered enzymes where E134 was changed to an aspartate or an alanine residue.

The specific activity of E134D-DapE was determined in the presence of L,L-SDAP, which is the natural substrate for this enzyme. Kinetic parameters for Zn(II)-loaded WT and E134D, DapE indicate that, in general, the effect on activity is due to a decrease in k_{cat} (Table 1) similar to that observed for AAP [19]. Interestingly, replacement of E134 with a residue that is still capable of transferring a proton or forming hydrogen bonds, such as aspartate, provided a DapE enzyme that remains active but exhibits only 0.09% of the observed WT DapE activity. The K_m value does not significantly change, suggesting that substrate interacts normally with the active site. Similar to WT DapE, E134D-DapE can be activated by several divalent first-row transition metal ions, including Co(II), Cd(II), and Mn(II) [24]. Replacement of E134 with an alanine residue results in a totally inactive enzyme. These data indicate that E134 is absolutely required for catalytic turnover even though it has been proposed not to function as a Zn(II) ligand.

The isothermal titration calorimetry measurements for Zn(II) binding to E134A-DapE and E134D-DapE provided K_d values of 0.62 and 1.3 μM for the first metal binding sites, respectively. These values are approximately 1.4 and approximately 2.9 times weaker than the observed K_d value for WT DapE. Interestingly, the first Co(II) binding event for E134A-DapE and E134D-DapE provided K_d values of 0.094 and 0.028 μM, which are approximately 5 and approximately 15.0 times stronger than the WT binding of Co(II). In the absence of X-ray crystallographic data, the observed changes in the K_d values for Co(II) versus Zn(II) are difficult to explain; however, they are likely the result of the preference of Co(II) for five- or six-coordinate geometries versus four- or five-coordinate for Zn(II). For the second metal binding events, Zn(II) binds to E134A-DapE and E134D-DapE with K_d values of 65.4 and 9.1 μM, respectively, while Co(II) binds to the second metal binding site with K_d values of 60.2 and 1.24 μM, respectively. Therefore, E134D and E134A perturb the second divalent metal binding site significantly more than the first, but both altered enzymes can still bind two divalent metal ions. The Gibbs free energy does not change significantly upon substitution of E134 by aspartate or alanine and is similar to that observed for WT DapE [19]. Interestingly, the entropic factor ($T\Delta S^0$) drops sixfold for both E134A-DapE and E134D-DapE for the first metal binding event, which is consistent with the large change in K_d. On the other hand, $T\Delta S^0$ increases significantly for the second Zn(II) binding event in the order E134A<E134D<WT DapE, suggesting a decrease in order around the second metal binding site.

Ionizations derived from plots of $\log(k_{cat}/K_m)$ versus pH correspond to ionizations of the free enzyme and free substrate [33, 34]. On the basis of the available kinetic data for WT DapE [10] and the kinetic and X-ray crystallographic data for AAP [19, 33, 35], a simple, two-site model was used to describe the observed changes in ionization states of active-site residues with changing pH (Scheme 1). K_m and k_{cat} values were previously reported for Zn(II)-bound WT DapE over the pH range 6–9 and a plot of $\log(k_{cat}/K_m)$ versus pH provided a bell-shaped curve with two inflections at pH 6.6 and 8.3 [10]. For E134D-DapE, plots of $\log(k_{cat}/K_m)$ versus pH likely form bell-shaped curves but this assertion cannot be made conclusively owing to our inability to obtain data points above pH 9.0. Fits of $\log(k_{cat}/K_m)$ for E134D-DapE provided a K_{E1} value of 6.4, while K_{E2} was estimated to be approximately 9.7. The K_{E1} value obtained for E134D-DapE matches well with that reported for WT DapE (K_{E1}=6.6), consistent with its assignment as the ionization of a metal-centered water molecule. Interestingly, the observed K_{E2} value has shifted to a more basic pH value by approximately 1 pH unit. While the K_{E2} value

reported here is simply an estimate, qualitatively, the log(k_{cat}/K_m) versus pH profile for E134D-DapE is clearly shifted to more basic pH values compared with that for WT DapE. The basic K_{E2} value suggests that an enzyme residue needs to be protonated for the substrate to bind. The presence of an ionizing group between pH 8.5 and 9.5 for WT DapE and E134D-DapE, respectively, suggests a basic enzyme-centered residue must be protonated. Given the number of carboxylic acid residues on L,L-SDAP the most likely candidate would be an active-site lysine residue involved in substrate binding.

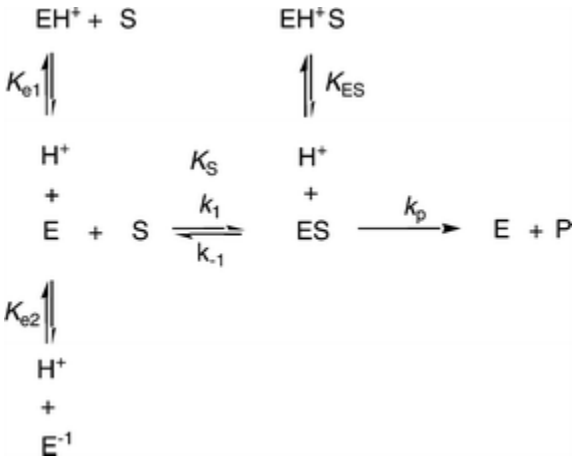

Scheme 1 Equilibrium scheme for substrate binding to different protein protonation states of *dapE*

For WT DapE, no change in k_{cat} was observed in the pH range 7.0–9, but a sharp drop in k_{cat} was observed below pH values of 7.0, which is identical to that observed for E134D-DapE. For WT DapE, a pK_a value of 6.6 was extracted from fits of the data, which matches well with the pK_a value of 6.4 observed for E134D-DapE. These data indicate that one ionizable group (pK_{ES}) must be deprotonated in the enzyme–substrate complex for catalysis to occur (Scheme 1), and that a similar process is responsible for the observed changes in k_{cat} for both the WT and the E134D-DapE enzymes. This pK_a value likely corresponds to the ionization of a metal-centered water molecule, as previously suggested [10]. A second alternative would be the ionization of a carboxylic acid in the enzyme–substrate complex, similar to AAP [19, 34]; however, a change in the rate-limiting step of the reaction cannot be entirely ruled out. If the observed pK_{ES} value at 6.4 is the ionization of a carboxylate residue (E134) that is required to be in an unprotonated form for the catalytic reaction to occur, one would expect to see a shift in this pK_a versus that of the WT enzyme. Since this shift is not observed, this pK_a value is likely the deprotonation of a metal-centered water molecule to a hydroxide as previously suggested [10].

Inspection of a plot of log(K_m) versus pH for E134D-DapE provided a K_{HS} value of 7.4. The observed inflection at pH 7.4 indicates that one group on the substrate or enzyme must be in the deprotonated form, resulting in increased substrate binding affinity, assisting enzyme–substrate complex formation. Assignment of these pK_a values is difficult but the pK_a value observed at pH 7.4 is likely due to one of the amino groups of L,L-SDAP since N-terminal amines typically exhibit pK_as in the range 7.5–10.0. As previously suggested, K_{E2} is either a substrate-centered amino group or an enzyme-centered lysine residue [35]. Alternatively, the large number of negatively charged residues residing in the active site may raise the pK_a of E134, suggesting that the observed pK_a at 7.4 is that of E134D; however, given the similarity of this pK_a with that of the substrate's amino groups, this assignment is unlikely.

To further examine the metal binding properties of E134A-DapE and E134D-DapE, electronic absorption spectra of the Co(II)-loaded forms of each altered enzyme were recorded. Upon the addition of 1 equiv Co(II) under anaerobic conditions, three resolvable *d–d* transitions in the 500–600-nm range (at λ_{max} ε=165–190 M^{-1} cm^{-1}) were observed for both E134A-DapE and E134D-DapE. Ligand-field theory predicts that optical transitions of

four-coordinate Co(II) complexes give rise to intense absorptions (ε>300 $M^{-1}\,cm^{-1}$) in the higher-wavelength region (625±50 nm) owing to a comparatively small ligand-field stabilization energy, while transitions of octahedral Co(II) complexes have very weak absorptions (ε<30 $M^{-1}\,cm^{-1}$) at lower wavelengths (525±50 nm). Five-coordinate Co(II) centers show intermediate features, i.e., moderate absorption intensities (50<ε<250 $M^{-1}\,cm^{-1}$) with several maxima between 525 and 625 nm [36, 37]. On the basis of the molar absorptivities and *d*–*d* absorption maxima of [Co_(E134A-DapE)] and [Co_(E134D-DapE)] the first metal binding site is likely pentacoordinate. However, very little absorbance increase is observed upon the addition of a second equivalent of Co(II), similar to the situation for WT DapE [24], suggesting that the second metal binding site is octahedral or a very distorted pentacoordinate geometry. Because the second Co(II) ion is weakly bound to E134A-DapE and E134D-DapE, an equilibrium exists between free and bound Co(II); therefore, the ε value (approximately 10 $M^{-1}\,cm^{-1}$) for the second Co(II) binding event is likely an underestimate of the actual value. Similar results have been reported for Co(II)-substituted AAP [26, 28, 38].

Taken with the optical absorption data, the EPR spectra of [Co_(E134A-DapE)] and [Co_(E134D-DapE)] are consistent with either a five- or a six-coordinate environment for the first Co(II) binding site. The absence of features due to $M_S = |\pm 3/2\rangle$ transitions render tetrahedral geometry unlikely, while the optical absorption coefficients would be unusually large for octahedral Co(II). The nonzero *E*/*D* value and the relatively large amounts of *g* and *A* strain suggest a geometry with similar electronic symmetry and orientational flexibility to that seen for five- or six-coordinate systems such as hexaaquo-Co(II). The lack of resolved hyperfine structure on the low-field line suggests coordination differences between the catalytic Co(II) ion in DapE and that in AAP. Interestingly, the signal is very distinct from that seen upon the addition of up to 1 equiv Co(II) to WT DapE [24]. The latter exhibits well-resolved resonances at g_{eff}=5.6 and g_{eff}=3.7, consistent with an isotropic *g* of 2.38 with *E*/*D*=0.1. The WT signal is very similar to the signal from the five-coordinate Co(II) ion in the cobalt-substituted *β*-lactamase, VanX [39]. Though the spin Hamiltonian parameters $g_{(x,y)}$ and *E*/*D* are similar for [Co_(DapE)] and [Co_(E134D-DapE)], the strain-dependent linewidths are clearly very different and suggest a level of geometric flexibility of the active-site metal ion of [Co_(E134D-DapE)] that is lacking in [Co_(DapE)]. The EPR data for [CoCo(E134A-DapE)] and [CoCo(E134D-DapE)] are similar to those of [CoCo(DapE)], AAP, and *Ec*MetAP-I and suggest that there is little change in the electronic symmetry of the catalytic Co(II) ion upon binding of the second Co(II) [24, 26–28]. These data do, however, indicate substantial line-broadening of the low-field line of the catalytic Co(II) ion and indicate an effect either on the precise coordination geometry of this metal ion or on the electronic properties owing to spin–spin interactions between the two Co(II) ions. The spectra for [CoCo(E134A-DapE)] and [CoCo(E134D-DapE)] are consistent with five- or six-coordinate Co(II) in the second site with relatively high axial electronic symmetry, though the spectra are not sufficiently well resolved to determine the parameters precisely. The spin density appears to account for all the added Co(II) and, therefore, strong exchange coupling is not likely between the two cobalt ions.

In conclusion, the data presented herein in combination with previously reported kinetic and spectroscopic reported for DapE establish, for the first time, that E134 is absolutely required for SDAP hydrolysis to occur. Since all of the active-site residues in AAP and CPG_2 are strictly conserved in DapE [10] and the as-purified DapE enzyme exhibits approximately 90% of its activity in the presence of one Zn(II) ion, similar to AAP [40], the proposed catalytic mechanism for AAP was used as a starting model for DapE [35]. Once substrate binding occurs at the DapE active site, the substrate carbonyl group likely binds to M1 and is activated for nucleophilic attack (Fig. 7). Deprotonation of the metal-bound water molecule to form a nucleophilic hydroxide moiety is consistent with the postulated pK_a of the metal-centered water molecule [10]. Once the metal-bound hydroxide has formed, it can attack the activated carbonyl carbon of the substrate, forming an η-1-μ-transition-state complex [29]. Solvent kinetic isotope effect studies yielded an inverse isotope effect that was explained by the attack of a Zn(II)-bound hydroxide on the amide carbonyl [10]. E134 may also provide a proton to the penultimate amino nitrogen, similar to that observed for AAP, returning it to its ionized state and thus

facilitating product release. Once the products have been released, a water molecule bridging the two metal ions is replaced.

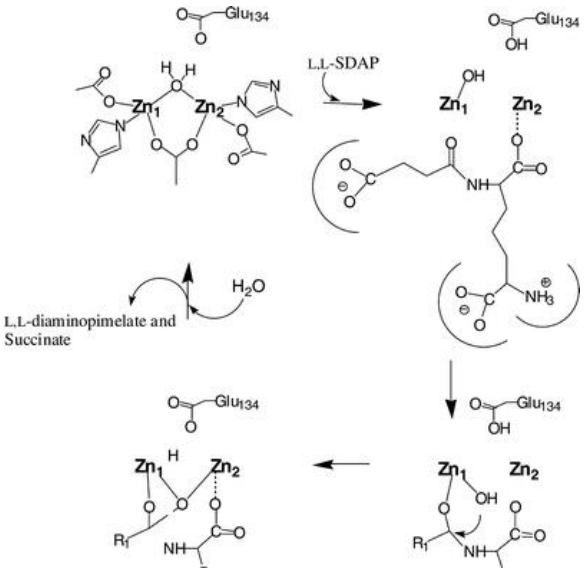

Fig. 7 Proposed catalytic mechanism for the DapE enzyme from *Haemophilus influenzae*

Abbreviations

AAP: Aminopeptidase from *Aeromonas proteolytica*
CPG$_2$: Carboxypeptidase G$_2$ from *Pseudomonas* sp. strain RS-16
DapE: *dapE*-encoded *N*-succinyl-L,L-diaminopimelic acid desuccinylase)
EcMetAP-I: Methionyl aminopeptidase from *Escherichia coli*
EPR: Electron paramagnetic resonance
E134: Glutamate-134
E151: Glutamate-151
HEPES: 4-(2-Hydroxyethyl)-1-piperazineethanesulfonic acid
mDAP: *meso*-Diaminopimelate
D,D-SDAP: *N*-Succinyl-D,D-diaminopimelate
L,L-SDAP: *N*-Succinyl-L,L-diaminopimelate
SDAP: *N*-Succinyl-diaminopimelic acid
Tricine: *N*-Tris(hydroxymethyl)methylglycine
Tris: Tris(hydroxymethyl)aminomethane
WT: Wild type

References

1. Prevention CfDCa (1995) MMWR Morb Mortal Wkly Rep 44:1–13
2. Snider DE, Raviglione M, Kochi A (1994) Tuberculosis: pathogenesis, protection, control. In: Bloom BR (ed) Global burden of tuberculosis. ASM Press, Washington, pp 3–11
3. Howe RA, Bowker KE, Walsh TR, Feest TG, MacGowan AP (1997) Lancet 351:601–602
4. Levy SB (1998) Sci Am 278:46–53
5. Chin J (1996) New Sci 152:32–35
6. Scapin G, Blanchard JS (1998) Adv Enzymol 72:279–325
7. Born TL, Blanchard JS (1999) Curr Opin Chem Biol 3:607–613
8. Girodeau J-M, Agouridas C, Masson M, Pineau R, LeGoffic F (1986) J Med Chem 29:1023–1030

9. Velasco AM, Leguina JI, Lazcano A (2002) J Mol Evol 55:445–459
10. Born TL, Zheng R, Blanchard JS (1998) Biochemistry 37:10478–10487
11. Karita M, Etterbeek ML, Forsyth MH, Tummuru MR, Blaser MJ (1997) Infect Immun 65:4158–4164
12. Pavelka MS, Jacobs WR (1996) J Bacteriol 178:6496–6507
13. Bouvier J, Richaud C, Higgins W, Bögler O, Stragier P (1992) J Bacteriol 174:5265–5271
14. Lipscomb WN, Sträter N (1996) Chem Rev 96:2375–2433
15. Vallee BL, Auld DS (1990) Biochemistry 29:5647–5659
16. Vallee BL, Auld DS (1993) Proc Natl Acad Sci USA 90:2715–2718
17. Vallee BL, Auld DS (1993) Biochemistry 32:6493–6500
18. Chevrier B, Schalk C, D'Orchymont H, Rondeau J-M, Moras D, Tarnus C (1994) Structure 2:283–291
19. Bzymek KP, Holz RC (2004) J Biol Chem 279:31018–31025
20. Gill SC, von Hippel PH (1989) Anal Biochem 182:319–326
21. D'souza VM, Holz RC (1999) Biochemistry 38:11079–11085
22. Bergmann M, Stein WH (1939) J Biol Chem 129:609–618
23. Lin Y, Myhrman R, Schrag ML, Gelb MH (1988) J Biol Chem 263:1622–1627
24. Bienvenue DL, Gilner DM, Davis RS, Bennett B, Holz RC (2003) Biochemistry 42:10756–10763
25. Javid-Majd F, Blanchard JS (2000) Biochemistry 39:1285–1293
26. Bennett B, Holz RC (1997) Biochemistry 36:9837–9846
27. D'souza VM, Bennett B, Copik AJ, Holz RC (2000) Biochemistry 39:3817–3826
28. Bennett B, Holz RC (1997) J Am Chem Soc 119:1923–1933
29. Cosper NJ, Bienvenue DL, Shokes J, Gilner DM, Tsukamoto T, Scott R, Holz RC (2004) J Am Chem Soc 125:14654–14655
30. Chevrier B, D'Orchymont H, Schalk C, Tarnus C, Moras D (1996) Eur J Biochem 237:393–398
31. Rowsell S, Pauptit RA, Tucker AD, Melton RG, Blow DM, Brick P (1997) Structure 5:337–347
32. Christianson DW, Lipscomb WN (1989) Acc Chem Res 22:62–69
33. Baker JO, Prescott JM (1983) Biochemistry 22:5322–5331
34. Segel IH (1993) Enzyme kinetics. Behavior and analysis of rapid equilibrium and steady-state enzyme systems. Wiley, New York
35. Holz RC (2002) Coord Chem Rev 232:5–26
36. Bertini I, Luchinat C (1984) Adv Inorg Biochem 6:71–111
37. Horrocks WD Jr, Ishley JN, Holmquist B, Thompson JS (1980) J Inorg Chem 12:131–141
38. Prescott JM, Wagner FW, Holmquist B, Vallee BL (1985) Biochemistry 24:5350–5356
39. Breece RM, Costello A, Bennett B, Sigdel TK, Matthews ML, Tierney DL, Crowder MW (2005) J Biol Chem 280:11074–11081
40. Prescott JM, Wilkes SH (1976) Methods Enzymol 45:530–543

Acknowledgements

The authors would like to thank Krzysztof P. Bzymek for helpful discussions. This work was supported by the National Science Foundation (CHE-0549221, R.C.H.) and the Medical College of Wisconsin Research Affairs Committee (B.B.). The Bruker ESP-300E EPR spectrometer was purchased with funds provided by the National Science Foundation (BIR-9413530) and XSophe was purchased with funds from the National Institutes of Health (NIH RR01008, B.B.).